Journal of Biomolecular NMR, 3 (1993) 577–595
ESCOM

J-Bio NMR 146

Two- and three-dimensional ^{31}P-driven NMR procedures for complete assignment of backbone resonances in oligodeoxyribonucleotides

Gregory W. Kellogg[a] and Barry I. Schweitzer[b,*]

[a]*Departments of Molecular Biophysics and Biochemistry and Chemistry, Yale University, New Haven, CT 06510-8064, U.S.A.*
[b]*Department of Pediatrics, Yale University, School of Medicine, 333 Ceder Street, New Haven, CT 06510-8064, U.S.A.*

Received 18 February 1993
Accepted 7 May 1993

Keywords: DNA; NMR; Assignment; Heteronuclear; HeteroTOCSY

SUMMARY

We describe a strategy for sequential assignment of ^{31}P and deoxyribose ^{1}H NMR resonances in oligodeoxyribonucleotides. The approach is based on ^{31}P–^{1}H J-cross-polarization (heteroTOCSY) experiments, recently demonstrated for the assignment of resonances in RNA [Kellogg, G.W. (1992) *J. Magn. Reson.*, **98**, 176; Kellogg, G.W. et al. (1992) *J. Am. Chem. Soc.*, **114**, 2727]. Two-dimensional heteroTOCSY and heteroTOCSY-NOESY experiments are used to connect proton spin systems from adjacent nucleotides in the dodecamer d(CGCGAATTCGCG)$_2$ entirely on the basis of through-bond scalar connectivities. All phosphorus resonances of the dodecamer are assigned by this method, and many deoxyribose ^{1}H resonances can be assigned as well. A new three-dimensional heteroTOCSY-NOESY experiment is used for backbone proton 4', 5' and 5" resonance assignments, completing assignments begun on this molecule in 1983 [Hare, D.R. et al. (1983) *J. Mol. Biol.*, **171**, 319]. Numerical simulations of the time dependence of coherence transfer aid in the interpretation of heteroTOCSY spectra of oligonucleotides and address the dependence of heteroTOCSY and related spectra on structural features of nucleic acids. The possibility of a generalized backbone-driven ^{1}H and ^{31}P resonance-assignment strategy for oligonucleotides is discussed.

INTRODUCTION

High-resolution ^{1}H NMR spectroscopy can be used to determine the three-dimensional (3D) structures of biopolymers in solution, including the local conformations of small oligonucleotides (Clore and Gronenborn, 1985; Reid, 1987; Van de Ven and Hilbers, 1988; Varani and Tinoco, 1991). All such projects begin with the assignment of proton resonances from multidimensional NMR spectra, followed by the measurement of nuclear Overhauser effects (NOEs) between

*To whom correspondence should be addressed.

proton resonance pairs and estimation of scalar coupling constants (Wüthrich, 1986). This information is then entered into minimization algorithms such as distance geometry and restrained molecular dynamics, from which a 3D structure is generated. In practice, resonance assignment is the most time-consuming step in the determination of a solution structure by NMR.

The standard strategy for nucleic acid resonance assignment (Feigon et al., 1983; Hare et al., 1983; Scheek et al., 1984) depends on the observation of sequential NOESY cross peaks predicted from structural models of double-helical DNA or RNA. This strategy is far from ideal. Nucleic acid sequences that adopt unusual structures or that contain lesions with altered conformation are among the most interesting candidates for study by NMR, yet the spectra of these molecules are the most difficult to assign. The problem is complicated further by the usual order of assignment. The sequential cross peaks in NOESY spectra of DNA and RNA result from exchangeable, aromatic and anomeric (H1') protons; these resonance assignments are heavily reinforced by the redundancy of information in double-helical regions. Resonance assignments of backbone protons (H3', H4', H5' and H5") are less well established, and in some cases are absent entirely. Partly as a consequence of this fact, the backbone conformations of many nucleic acid solution structures are underdetermined by NMR data (Metzler et al., 1990; Kim et al., 1992). More complete and reliable backbone resonance assignments are needed to improve the quality of solution structures.

Pardi et al. (1983) were the first to suggest a backbone-oriented assignment strategy, using a combination of 2D ^{1}H–^{1}H and ^{1}H–^{31}P spectroscopy. Their approach was to relate H3'–H4', H4'–H5' and H4'–H5" cross peaks of DQF-COSY spectra to H3'–^{31}P and H5',H5"–^{31}P cross peaks of 2D ^{1}H–^{31}P correlation spectra, thereby connecting adjacent deoxyribose spin systems. Because a four-bond coupling between H4' and the 5'-attached phosphorus can sometimes be observed in double-helical nucleic acids (Altona, 1982; Marion and Lancelot, 1984), this assignment strategy can be used in the absence of resolved H5' and H5" resonances, provided that H3'–H4' resonance cross peaks are resolved. Use of the phosphorus correlation method for sequential ^{1}H resonance assignment is limited to fairly small oligonucleotides, though proton-detected correlation methods have shown impressive results (Sklenar et al., 1986; Sklenar and Bax, 1987). For larger molecules, or as a general-purpose alternative, site-specific ^{17}O labeling of phosphoryl oxygens can be used to assign ^{31}P resonances (Connolly and Eckstein, 1984), and those assignments can then be used to derive ^{1}H assignments from ^{1}H–^{31}P correlations.

The phosphorus correlation method (Pardi et al., 1983) is preferable in principle to NOESY-based assignment methods. It is severely limited, however, by the need for good proton resolution in the crowded sugar-proton region of DQF-COSY spectra. This limitation might be overcome by correlating ^{31}P resonances with clearly resolved ^{1}H resonances, as has been attempted for DNA molecules by two groups, using a combination of HOHAHA and ^{1}H–^{31}P INEPT spectroscopy (Hiroaki and Uesugi, 1989; Zagorski and Norman, 1989). Both groups observed weak correlations between remote (H1',H2'/H2") proton resonances and phosphorus resonances, and Hiroaki and Uesugi noted the presence of weak, sequential correlations in the H3', H5' region of

---

Abbreviations: TOCSY, Total Correlation Spectroscopy; NMR, Nuclear Magnetic Resonance; FID, Free Induction Decay; COSY, Correlation Spectroscopy; heteroCOSY, Heteronuclear Correlation Spectroscopy; NOESY, Nuclear Overhauser Effect Spectroscopy; HMQC, Heteronuclear Multiple Quantum Coherence; HSQC, Heteronuclear Single Quantum Coherence.

a 2D ^{1}H–^{31}P correlated spectrum of a trinucleotide. Proton-detected ^{1}H–^{31}P heteronuclear RELAY experiments have been demonstrated on mononucleotides (Field and Messerle, 1985, 1986). More recently, heteronuclear J cross-polarization spectroscopy (heteroTOCSY) (Bearden and Brown, 1989; Artemov, 1991; Morris and Gibbs, 1991) was applied to a double-stranded oligo*ribo*nucleotide with proton detection (Kellogg, 1992a), and shown to correlate ^{31}P resonances with several ^{1}H resonances (including H2') on adjacent ribose rings. An extension of the heteroTOCSY experiment to a 2D heteroTOCSY-NOESY experiment produced correlations in a double-stranded oligoribonucleotide between ^{31}P resonances and H1' resonances from residues at the 5' side of the phosphate and complete sequential correlations between ^{31}P resonances and aromatic ^{1}H resonances (Kellogg et al., 1992). It was possible in this case to obtain sequential ^{31}P assignments without prior information about ribose ^{1}H assignments.

The applications of heteroTOCSY experiments to oligodeoxyribonucleotides are explored in this paper, using the much-studied dodecamer d(CGCGAATTCGCG)$_2$, a parental system for future studies of sugar–phosphate lesions in oligonucleotides. These experiments are shown to yield *through-bond* sequential assignment of ^{31}P resonances in DNAs, independent of any prior knowledge of ^{1}H assignments and without any requirement for ^{1}H NOEs between aromatic and anomeric protons. Through-bond sequential assignment cannot be expected in all cases, however, and will depend on structural and dynamic properties of the nucleic acid. Computer simulations of magnetization transfer in the heteroTOCSY experiment have been carried out to explore this dependence and to offer some guide to interpretation in the light of current understanding of nucleic acid structure. Finally, it is demonstrated that 2D and 3D heteroTOCSY-NOESY experiments can give additional sequential correlations which reinforce ^{31}P assignments and provide complete assignments of backbone ^{1}H resonances, including previously unresolved H5',H5" resonances. The 3D experiment is exceptional in this regard; heteronuclear 3D NMR (Fesik and Zuiderweg, 1988; Marion et al., 1989) has been shown to be feasible for unlabeled nucleic acids.

The heteroTOCSY family of experiments forms the basis for a ^{1}H and ^{31}P resonance-assignment strategy for nucleic acids that is complementary to traditional approaches, because it is driven by the assignment of backbone nuclear resonances, not by the assignment of aromatic and anomeric resonances. Because of the sensitivity of ^{31}P chemical shifts to backbone conformation, this strategy is expected to be most informative in regions of unusual structure. Unambiguous assignment of these resonances should provide additional constraints for the generation and refinement of 3D structures, and thus improve their quality.

MATERIALS AND METHODS

Sample preparation

The DNA dodecamer d(CGCGAATTCGCG)$_2$ was synthesized on a 10-μM scale using standard solid-phase phosphoramidite techniques. The trityl-on deprotected DNA was purified via an HPLC protocol which removes failure sequences, the trityl group, and nonfailure contaminating DNAs on a single column. DNA in 1 ml TEAB was loaded onto a 10 × 100 mm Aquapore Octyl HPLC column (Brownlee), equilibrated in 85% TEAA/15% acetonitrile. The column was washed with 30 ml 85% TEAA/15% acetonitrile, and subsequently with 20 ml 100% TEAA, followed by removal of the trityl group with 20 ml 0.5% trifluoroacetic acid (TFA) in water and elimination of TFA with 20 ml 100% TEAA. The pure (> 98%) dodecamer was then eluted with a linear

gradient of 0–50% acetonitrile. Fractions containing the purified DNA were pooled, dialyzed twice against Chelex-100 (BioRad), and lyophilized to dryness. The lyophilized DNA was dissolved in 0.4 ml of buffer, containing 50 mM NaCl, 0.5 mM EDTA, 50 mM sodium phosphate (pH 7.0), and repeatedly lyophilized to dryness, first from the aqueous buffer and then from 99.96% D_2O. Finally, 0.4 ml of 99.996% D_2O was added to give a duplex concentration of 6 mM.

NMR spectroscopy

All NMR experiments were carried out on a Bruker AM500 spectrometer (500.13 MHz for protons), modified as described below, operating in the inverse mode. The sample temperature was regulated at 303 K for all experiments. The proton-detected ^{31}P–^{1}H heteronuclear correlation experiment was carried out using the pulse scheme of Sklenar et al. (1986). Phase-sensitive data were collected in the hypercomplex mode of States et al. (1982). HeteroTOCSY, hetero/homoTOCSY, heteroTOCSY-NOESY and hetero/homoTOCSY-NOESY experiments were carried out using the pulse schemes shown in Fig. 1. In these experiments, four power settings on two channels were used; the decoupler channel was used for the proton pulses at high power for the presaturation sequence and at a lower power for the remaining pulses. The transmitter (set to ^{31}P) was equipped with a fast (2 μs) low-power switch and a fast-switch linear amplifier with a resolution of 0.1 dB. The transmitter power level was adjusted manually to meet the Hartmann–Hahn matching condition during the contact time of each experiment (Kellogg, 1992a). Correction for a differential timing between the switch and the actual output was made in the Bruker microprogram. The effectiveness of Hartmann–Hahn contact was estimated by measuring the sensitivity of cross-polarization to maladjustment of transmitter power and frequency offset. Optimization of transmitter output to within 0.5 dB of a perfect match was found to be adequate and could be achieved using pulse-width measurements, or by calibrating the power. The necessary modifications to the spectrometer were made by Mr. Peter Demou and Dr. Ben Bangerter of the Yale Chemical Instrumentation Center. Data were recorded in the phase-sensitive mode with time-proportional phase incrementation (TPPI) (Marion and Wüthrich, 1983). In the NOESY variants of the heteroTOCSY experiments, the time of the NOESY mixing period was subjected to a ± 8% random variation to reduce interference from zero-quantum coherence. A homospoil pulse of 20 ms duration was applied at the beginning of this mixing period.

NMR data processing

NMR data were processed using the program FELIX 2.05 (Hare Research, Inc.). In the ^{31}P–^{1}H heteroCOSY, heteroTOCSY, hetero/homoTOCSY, heteroTOCSY-NOESY and hetero/homoTOCSY-NOESY experiments, the t_1 dimension was zero-filled to 256 points. No zero-filling was used in the t_2 dimension. In the 3D heteroTOCSY-NOESY experiment, the t_1 (^{31}P) dimension was zero-filled to 128 points, the t_2 (^{1}H) dimension to 512 points, and no zero-filling was used in the t_3 (^{1}H) dimension. In the ^{31}P–^{1}H heteronuclear correlation experiment, the dataset was apodized with an unshifted sine bell in both dimensions, prior to Fourier transformation. In the heteroTOCSY and related experiments, datasets were apodized with a squared sine-bell window shifted 60° in the t_2 dimension and with a sine-bell window shifted 30° in the t_1 dimension, prior to Fourier transformation; t_1 ridges were attenuated by multiplying the first t_1 slice by 0.5 (Otting et al., 1985). The 3D heteroTOCSY-NOESY dataset was apodized with squared sine-bell functions shifted by 60°, 45° and 45° in the t_3, t_2 and t_1 dimensions, respectively. The first time point of each

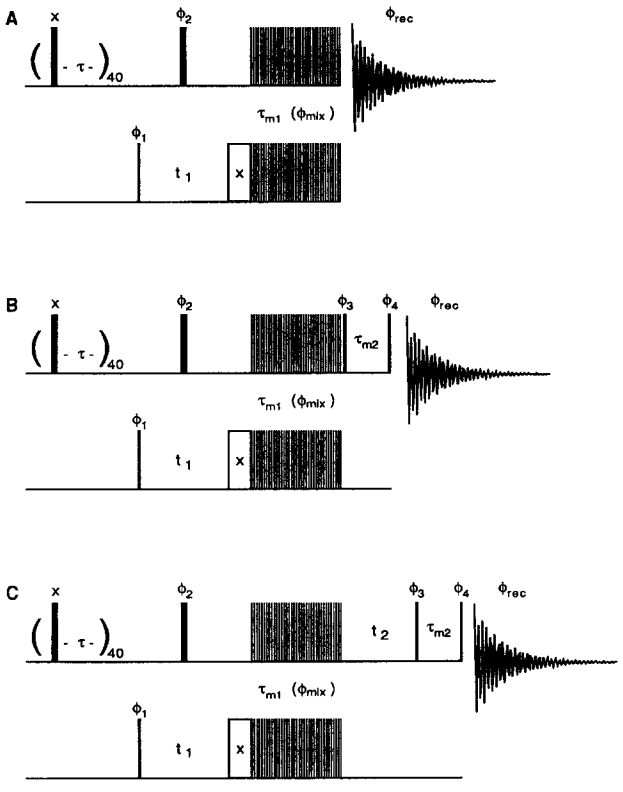

Fig. 1. Pulse sequence diagrams for (A) 2D heteroTOCSY; (B) 2D heteroTOCSY-NOESY; and (C) 3D heteroTOCSY-NOESY experiments. Thin vertical lines represent 90° pulses, thick lines represent 180° pulses. Protons are presaturated with a series of 40 high-power 180° pulses, separated by 50-ms delays (τ in the figure). The refocusing pulse ϕ_2 is a composite 90°/2(x)-180°(y)-180°/2(x) low-power pulse, the low power being required by hardware timing limitations. The hatched boxes represent Hartmann–Hahn matched DIPSI-2 (Shaka, 1988) pulse mixing sequences for cross-polarization. The phase cycling for the heteroTOCSY is as follows: ϕ_1 = (y,−y) + TPPI; ϕ_{mix} = x, modulated by DIPSI-2; ϕ_{rec} = y,−y; the pulses in ϕ_2 are alternated after every two scans. The phase cycling for the heteroTOCSY-NOESY is as follows: ϕ_1 = (−y,y) + TPPI; ϕ_{mix} = x, modulated by DIPSI-2; ϕ_3 = y; ϕ_4 = 4x, 4(−x), 4y, 4(−y); ϕ_{rec} = 2(y,−y), 2(−y,y), 2(−x,x), 2(x,−x); the pulses in ϕ_2 are alternated after every two scans. The hetero/homo versions of the above experiments differ only in that the DIPSI-2 mixing sequence on ^{31}P is stopped partway through the mixing period, and the phases of the remaining ^1H mixing pulses are shifted by $\pi/2$. The 3D heteroTOCSY-NOESY is similar to the 2D experiment, except for an additional incremental delay between the end of the mixing sequence and the first pulse of the NOESY sequence; furthermore, the basic phase cycling is shortened so that ϕ_4 is 4x, 4(−x), and ϕ_{rec} is 2(y,−y), 2(−y,y). To obtain pure phase quadrature data in t_2, ϕ_1, ϕ_2 and the entire DIPSI-2 sequence including the trim pulse were incremented by TPPI.

dimension was estimated by linear prediction. Phosphorus resonances are referenced to an external sample of trimethylphosphate, and proton resonances to an external sample of sodium-2,2-dimethyl-2-silapentane-5-sulfonate in a buffer identical to that of the NMR sample.

Computer simulations

The time dependence of coherence transfer was simulated for idealized spin systems using the program ZTOCSY (Cavanagh et al., 1990), generously provided by Mark Rance (Scripps Res. Clinic). This program computes the influence of an isotropic mixing Hamiltonian on the evolu-

tion of coupled spins in the absence of relaxation. To handle heteronuclear spin systems without introducing a time-dependent Hamiltonian, the program was used as provided, except that heteronuclear coupling constants were scaled by 50% to account for the reduced rate of polarization transfer, relative to homonuclear transfer steps (Müller and Ernst, 1979; Braunschweiler and Ernst, 1983). For each simulation, 512 expectation values for observable magnetization were calculated in 1-ms increments. To simulate dinucleotide fragments, where inclusion of all the spins would exceed the capacity of the program, the 1', 5' and 5" protons were removed from the 5' residue, and the 1, 2' and 2" protons were removed from the 3' residue, leaving a total of nine spins. Mononucleotide simulations suggested that this is reasonable for the mixing times considered. Deoxyribose scalar coupling constants were calculated for various pseudorotation angles assuming a maximum pucker amplitude Φ_m of 36°, using the modified Karplus equation and parameters of Van Wijk et al. (1992). These are the most recent descendants of the Haasnoot equation (Haasnoot et al., 1980). Backbone coupling constants were fixed at the 'canonical' values for A or B DNA as described by Altona (Altona, 1982; Arnott et al., 1980).

RESULTS

Phosphorus–proton correlations in DNA

Phosphorus resonances can have ^{1}H correlates on the preceding (5'), the following (3'), or both deoxyribose neighbors, and deoxyribose protons can have ^{31}P correlates on the preceding (5'), the following (3'), or both neighboring phosphates. For convenience and clarity we will adopt the following convention. A heteronuclear correlation will be considered *intranucleotide* if it involves a proton resonance of a deoxyribose that precedes the phosphorus in question, and *internucleotide* if it does not. A correlation will be classified as *sequential* if both intranucleotide and internucleotide correlations are seen for either (i) a single proton resonance and resonances from both adjacent phosphates, or (ii) a single phosphorus resonance and proton resonances of the same type from both adjacent deoxyribose systems.

Figure 2A shows the entire spectrum from an inverse-detected ^{31}P–^{1}H heteronuclear correlation (heteroCOSY) experiment, carried out on the DNA dodecamer (Sklenar et al., 1986). The heteroCOSY experiment gives antiphase multiplet correlations between an ^{31}P and directly coupled protons: these include H3', H5', H5" and any four-bond coupled protons. The latter category can include H4' resonances from either deoxyribose neighbor, and H2'/H2" from the preceding nucleotide, but is usually restricted to the H4' of the following nucleotide in double-helical nucleic acids. In the spectrum of Fig. 2A, direct correlations to H3', H4', H5' and H5" resonances are the only ones seen. As illustrated in Fig. 2B, however, additional correlations appear in a heteroTOCSY spectrum (Kellogg, 1992a); some H1' and H2'/H2" correlations are seen, and the H3', H4', H5'/H5" region is much more crowded. This is a consequence of the simultaneous net coherence transfer of both heteronuclear and homonuclear coherences (Bearden and Brown, 1989; Zuiderweg, 1990). In addition, all cross peaks are absorptive and in-phase, and the ^{31}P dimension is decoupled from protons and thus better resolved than in the heteroCOSY spectrum.

The heteroTOCSY spectra of DNA and RNA show qualitative differences

In a heteroTOCSY spectrum, each internal phosphorus resonance of an RNA or DNA has possible intranucleotide correlates via the H3' sugar proton and internucleotide correlates via the

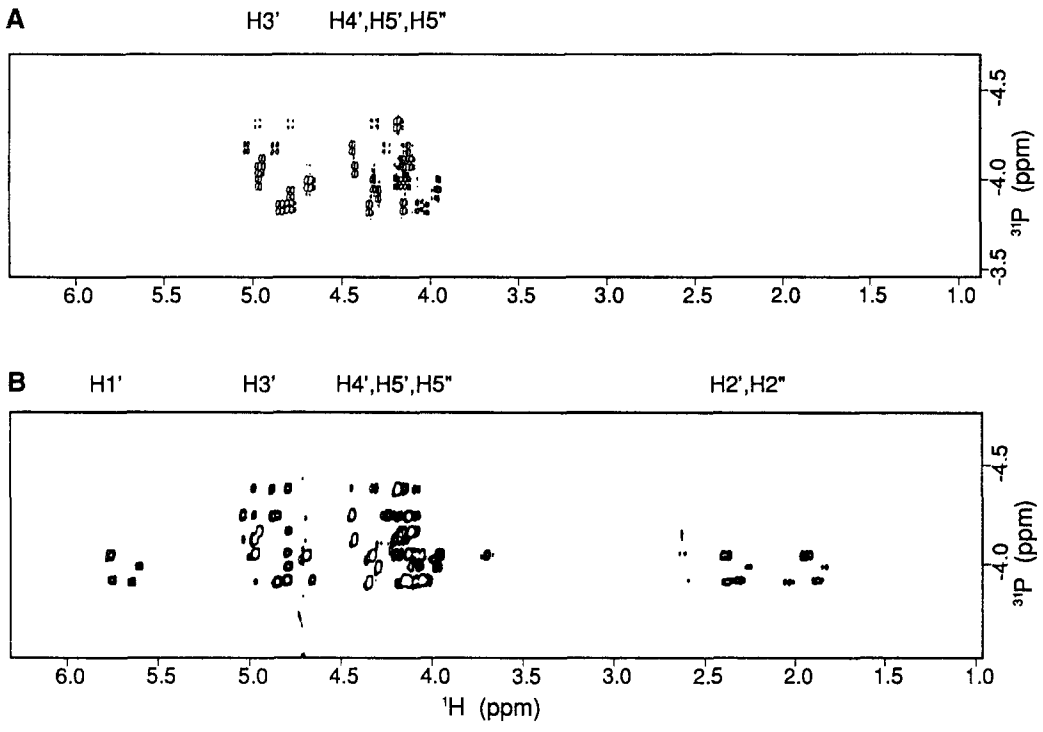

Fig. 2. ^{31}P–^{1}H correlations in d(CGCGAATTCGCG)$_2$ using a 2D heteronuclear correlation experiment or a 2D hetero-TOCSY experiment. (A) ^{1}H-detected heteronuclear correlation NMR spectrum of d(CGCGAATTCGCG)$_2$ at 303 K. The experiment was carried out with the following parameters: the 90° pulse width and sweep width for phosphorus were 11.5 μs and 252.5 Hz, respectively; the proton 90° pulse width and sweep width were 10 μs and 5000 Hz, respectively. The data were acquired with 1024 points in t_2 and with 800 transients for each of 40 complex t_1 points. The data were processed as described in Materials and Methods. Both positive and negative contours are drawn. (B) HeteroTOCSY spectrum of d(CGCGAATTCGCG)$_2$ at 303 K. The experiment was carried out as described in Materials and Methods, with the following parameters: the sweep width for phosphorus was 252.5 Hz, the proton offset and sweep width was 2674 Hz. The high-power 90° pulse widths for phosphorus and proton were 11.5 and 8.9 μs, respectively, while the low-power pulse width for both phosphorus and proton was 62.5 μs. The mixing times were 125 ms each. The data were acquired with 1024 points in t_2 and with 500 transients for each of 60 t_1 points. The data were processed as described in Materials and Methods. Only positive contours are drawn.

H5'/H5" and H4' protons. In the case of A-form RNA, the heteroTOCSY experiment transfers phosphorus magnetization efficiently from H3' to H4' and to H2', whereas three-step transfer via H3' to H5'/H5" or H1' protons is less efficient (Kellogg, 1992a). On the 3' side of the phosphorus, polarization transfer by heteroTOCSY is limited in double-helical RNA to directly coupled protons. In DNA oligonucleotides, on the other hand, transfer of coherence from an internal phosphorus to the H5'/H5" and H4' protons on its 3' side is more efficient than in RNA oligonucleotides. The presence of sequential cross peaks in the H3' region of the heteroTOCSY spectrum shown in Fig. 3A is evidence for this. The sequential correlations in this spectrum indicate that magnetization from a single phosphorus nucleus in DNA can be transferred to the H3' proton on the preceding residue, as in RNA, and also to the H5'/H5", H4', and eventually the H3' proton on the following residue. One such sequential H3' correlation is marked in Fig. 3A; it links residues

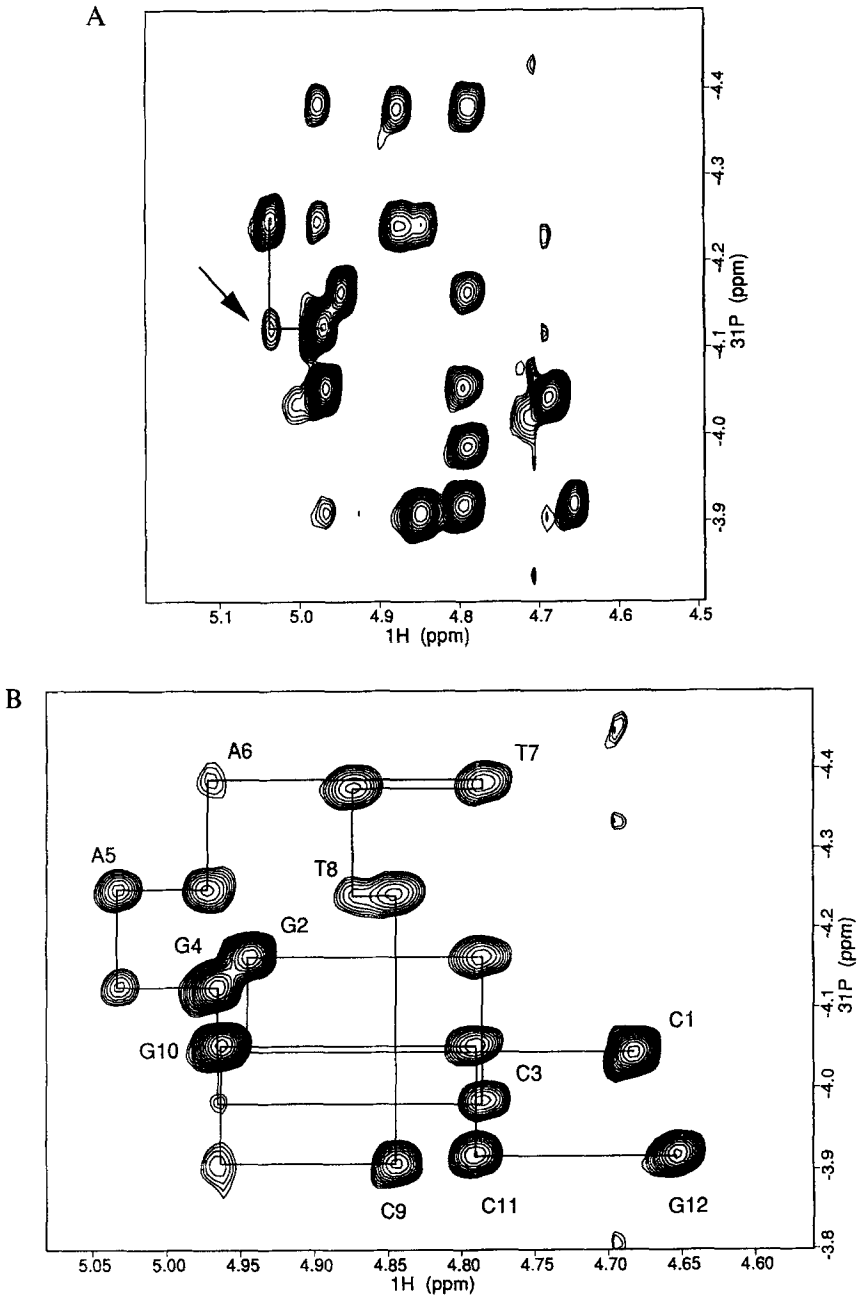

Fig. 3. Sequential ^{31}P–H3' correlations in d(CGCGAATTCGCG)$_2$ using a 2D heteroTOCSY experiment or a 2D hetero/homoTOCSY experiment. (A) Expanded H3' region of the heteroTOCSY spectrum of d(CGCGAATTCGCG)$_2$ shown in Fig. 2B. The arrow marks a sequential cross peak between the ^{31}P–H3' correlations of dG4 and dA5, connected by solid lines. (B) Expanded H3' region of the hetero/homoTOCSY spectrum of d(CGCGAATTCGCG)$_2$. Aquisition parameters were identical to those of Fig. 3A, with the exception that the heteronuclear mixing time was 100 ms, while the proton mixing sequence continued for an additional 75 ms. The sequential connectivities are traced with a solid line. Each of the intraresidue ^{31}P–H3' cross peaks is labeled with the residue name.

dG4 and dA5. Similar cross peaks can be seen for all other internucleotide phosphates, with the exception of the one between dC3 and dG4.

The sequential cross peaks in the heteroTOCSY spectrum of Fig. 3A allow an almost complete assignment of the dodecamer's phosphate backbone via the H3' correlations. In an effort to cross the gap between dC3 and dG4 we prolonged the mixing period in the heteroTOCSY experiment, hoping that this would extend coherence transfer to the H3' protons of dG2 and dG4 in just the way extending a homonuclear TOCSY mixing time allows assignments of H5'/H5" in DNA (Glaser et al., 1989). Unfortunately, extending the mixing period in the heteroTOCSY experiment past 125 ms caused sample heating. For this reason, we designed a variant of the heteroTOCSY, called hetero/homoTOCSY, in which the ^{31}P irradiation is terminated midway through the mixing period. This simple modification enabled us to use total mixing times of 175 ms without appreciable sample heating. As Fig. 3B shows, it allowed us to obtain a full set of ^{31}P assignments by tracing H3' correlations. The ^{31}P assignments are given in Table 1. These assignments agree with those previously published for this DNA duplex (Ott and Eckstein, 1985; Sklenar et al., 1986), except for minor shifts due to different experimental conditions. The assignments of Ott and Eckstein were made via ^{17}O labeling, and thus required a separate sample for each resonance assignment.

In a hetero/homoTOCSY experiment, a HOHAHA pulse sequence is added to the mixing period of a heteroTOCSY experiment, improving the sensitivity of the experiment. This is evident both in the completeness of the sequential connectivities in the H3' region and in the signal-to-noise ratio in the H2'/H2" region (data not shown). Several transfer steps are necessary for a sequential H3' correlation: coherence must be transferred first to the H5'/H5" and H4' protons and then relayed to H3' protons. Such remote cross peaks are weak, but can be observed provided sufficient intensity remains after transverse relaxation during the mixing period. The hetero/homoTOCSY pulse sequence was probably helpful in this respect, since we were able to switch the phase of the mixing pulses by 90° for the HOHAHA part, thereby slowing the effective relaxation of remaining coherence (Bax and Davis, 1985; Kellogg, 1992b).

TABLE 1
^{31}P CHEMICAL SHIFTS OF DINUCLEOSIDE PHOSPHATES IN $d(CGCGAATTCGCG)_2$ AT 303 K

Position	Dinucleoside step	Chemical shift (ppm)
1	d(CpG)	−4.04
2	d(GpC)	−4.16
3	d(CpG)	−3.98
4	d(GpA)	−4.11
5	d(ApA)	−4.24
6	d(ApT)	−4.37
7	d(TpT)	−4.37
8	d(TpC)	−4.23
9	d(CpG)	−3.90
10	d(GpC)	−4.04
11	d(CpG)	−3.91

Phosphorus positions are numbered from the 5' end. Chemical shifts are taken from a heteroTOCSY-NOESY experiment and are given relative to DSS.

Differences between DNA and RNA spectra persist in a 2D heteroTOCSY-NOESY

For RNA duplexes the addition of a NOESY sequence to the heteroTOCSY experiment correlates each ^{31}P resonance to aromatic proton resonances at both its 5' and 3' sides (Kellogg et al., 1992). The heteroTOCSY-NOESY experiment can thus be used to assign sequentially all ^{31}P resonances, as well as the H8 and H6 resonances in RNA oligonucleotides. When applied to DNA oligonucleotides, however, the 2D heteroTOCSY-NOESY experiment produces neither complete nor sequential ^{31}P correlations to aromatic protons (see Fig. 4). Intranucleotide ^{31}P correlations to aromatic protons are observed for less than half of the residues in the dodecamer, and only one internucleotide correlation (between dG10 and dC11) is seen. A hetero/homo-TOCSY-NOESY spectrum is not significantly different in this region (not shown).

The anomeric proton region of the 2D heteroTOCSY-NOESY spectrum (Fig. 5) is much more promising than the aromatic region. In the anomeric region, a complete set of sequential ^{31}P–^{1}H connectivities is observed; H1' resonances can be assigned and ^{31}P resonance assignments can be confirmed on this basis. In heteroTOCSY spectra obtained with this sample, the only sequential anomeric cross peak seen is the one between residues T8 and dC9; intranucleotide anomeric cross peaks are observed for all residues except dA6 (not shown). The intranucleotide ^{31}P–H3' cross peak for residue dA6 is very weak in both the heteroTOCSY and heteroTOCSY-NOESY spectra of the dodecamer (Fig. 3), and the ^{31}P–H1' cross peak for this residue is very weak in the heteroTOCSY-NOESY experiment (Fig. 5). This is probably a consequence of the small $^{3}J_{P-H3'}$ value for this residue (Sklenar and Bax, 1987).

When intranucleotide ^{31}P–H3' correlations are weak in heteroTOCSY spectra, as for residue dA6, sequential ^{31}P assignments can be obtained from the anomeric region of a heteroTOCSY-NOESY spectrum. These can then be used to resolve remaining ambiguities. This possibility arises because the heteroTOCSY-NOESY uses intranucleotide NOEs to establish internucleotide connectivities (vide infra). The 2D heteroTOCSY-NOESY experiment, combined with the

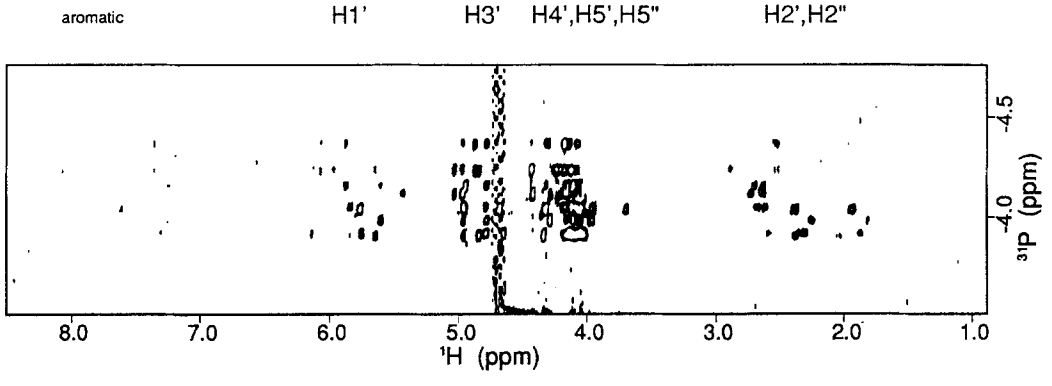

Fig. 4. 2D heteroTOCSY-NOESY spectrum of d(CGCGAATTCGCG)$_2$ at 303 K. The experiment was carried out as described in Materials and Methods with the following parameters: the sweep widths for ^{31}P and ^{1}H were 252.5 and 3816.8 Hz, respectively. The high-power 90° pulse widths for phosphorus and proton were 11.5 and 9 μs, respectively. The low-power pulse width for phosphorus and proton were both 62.5 μs. The TOCSY mixing sequence was 125 ms, and the NOESY mixing period was 300 ms (including the homospoil pulse). The data were acquired with 2048 points in t_2 and with 800 transients for each of 60 t_1 points. The data were processed as described in Materials and Methods. Only positive contours are drawn.

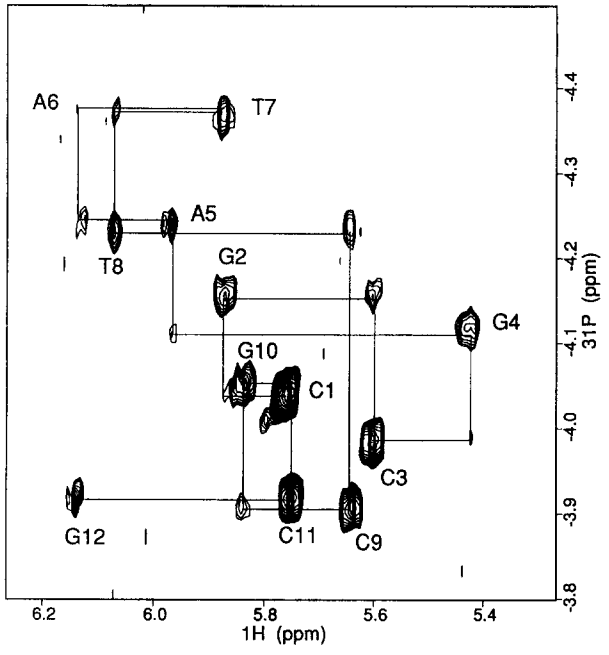

Fig. 5. Sequential ^{31}P–H1' correlations in d(CGCGAATTCGCG)$_2$ using a 2D heteroTOCSY-NOESY experiment. The H1' region from the heteroTOCSY-NOESY spectrum shown in Fig. 4 is expanded here. The sequential connectivities are traced with a solid line. Each of the intraresidue ^{31}P–H1' cross peaks is labeled with the residue name.

heteroTOCSY itself, can thus be used for simultaneous sequential assignment of ^{31}P, H3' and H1' resonances in DNA.

The upfield H2'/H2" region of the heteroTOCSY-NOESY experiment gives qualitatively similar information to that of the anomeric region, with both intranucleotide and internucleotide connectivities (data not shown). These data could be used in conjunction with the anomeric data to resolve assignment ambiguities.

A 3D heteroTOCSY-NOESY experiment

HeteroCOSY, heteroTOCSY and 2D heteroTOCSY-NOESY experiments produce ^{31}P correlations with H4' and H5'/H5" protons in DNA (Figs. 2 and 4), but as in RNA, the H4' and H5'/H5" proton resonances are difficult to resolve. A 3D version of the heteroTOCSY-NOESY experiment, however, gives excellent resolution in this region and provides a powerful approach for assigning these protons. Figure 6 shows one slice of a 3D spectrum, perpendicular to the phosphorus dimension at the frequency of the dC1/dG2 and dG10/dC11 phosphorus resonances. The diagonal peaks represent coherence which has been transferred to deoxyribose protons during the heteroTOCSY mixing period, whereas cross peaks represent magnetization which has undergone additional (incoherent) transfer during the NOESY mixing period.

Several features of this spectrum are remarkable. First, the cross peaks are quite strong, despite the fact that the number of scans per FID is one percent of that in the corresponding 2D spectrum. Second, as in the 2D heteroTOCSY and heteroTOCSY-NOESY experiments, sequen-

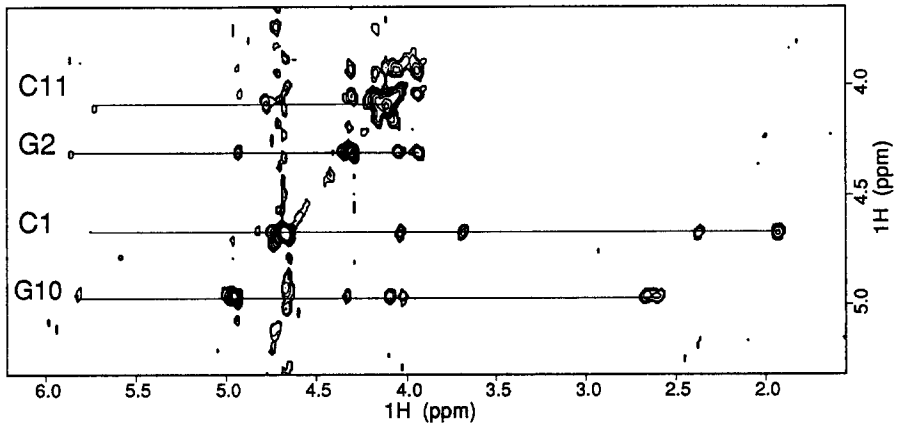

Fig. 6. Cross-sectional plane perpendicular to $\omega_1 = -4.06$ ppm in the 3D heteroTOCSY-NOESY spectrum of d(CGCGAATTCGCG)$_2$ at 303 K. The experiment was carried out as described in Materials and Methods with the following parameters: the sweep widths were 252 Hz (ω_1,^{31}P), 3108 Hz (ω_2,^{1}H) and 3816.8 Hz (ω_3,^{1}H). The pulse widths were roughly the same as in other experiments. The mixing times were 45 ms (τ_{m1}) and 300 ms (τ_{m2}, including the homospoil pulse). Twenty four, 90, and 512 complex points were acquired in the t_1, t_2 and t_3 dimensions, respectively. Eight transients (with two dummy scans) were acquired for each FID. The total measuring time was 72 h. The data were processed as described in Materials and Methods. Only positive contours are drawn. Horizontal lines connecting a set of deoxyribose correlations are drawn through the H3' frequencies (ω_2) of dC1 and dG10 and the H4' frequencies of dG2 and dC11.

tial correlations to the 3' residue are observed, here at the ω_2 frequency of the H4' proton at the 3' side of the phosphorus. Third, in this and other slices through the phosphorus dimension, clearly resolved cross peaks can be observed for all backbone protons on the deoxyribose ring. (Additionally, almost all H2' and H2" resonances, and most H1' resonances, are observed.) Of special note is the clear resolution of H5' and H5" cross peaks in this spectrum. Assignment of these resonances by conventional homonuclear experiments is often precluded by severe spectral overlap in nucleic acids of this size, but in 3D heteroTOCSY-NOESY spectra, individual H5' and H5" resonances can be resolved. Examples of this resolution can be seen in Fig. 6, in which individual H5' and H5" resonances can be observed for residue dG10 and for the sequential correlations at dG2. The resolution and spectral simplification afforded by this experiment allow complete and unambiguous assignment of all backbone (i.e. H3', H4' and H5'/H5") resonances in this sequence; these assignments are given in Table 2. For the same reason, where only one H5' resonance is observed we assign the H5'/H5" resonances as degenerate.

DISCUSSION

Lack of information about backbone distances and torsion angles is a serious barrier to the accurate determination of DNA structures by NMR (Nilges et al., 1987; Metzler et al., 1990; Kim et al., 1992). Useful information about backbone conformation, specifically the C4'-C3'-O3'-P torsion angle ε, can be obtained by measuring $^3J_{H3'-P}$ coupling constants, using 2D ^{1}H/^{31}P J-resolved experiments (Sklenar and Bax, 1987). In addition, Gorenstein and co-workers have found a strong correlation between variations in the chemical shifts of phosphorus resonances in

oligodeoxyribonucleotides and α and ζ torsion angles of the deoxyribose phosphate backbone (Schroeder et al., 1987; Gorenstein et al., 1988; Roongta et al., 1990).

Unfortunately, of the resonances in NMR spectra of DNA and RNA, ^{31}P and backbone ^{1}H resonances are the most difficult to assign. Assignment of ^{31}P resonances is likely to remain a critical stage in the investigation of nucleic acid structures by NMR. The reason is that, if we confine ourselves to considering ^{1}H resonances, each (deoxy)ribose is an isolated spin system. While multidimensional approaches combined with ^{13}C labeling will certainly improve the speed and reliability of proton resonance assignment within each sugar ring (Nikonowicz and Pardi, 1992a,b; Pardi and Nikonowicz, 1992), adjacent deoxyribose spin systems remain separated by four covalent bonds if the phosphorus is not included. Internucleotide NOEs are required, therefore, as long as (deoxy)ribose resonance assignment depends on ^{1}H–^{1}H and ^{1}H–^{13}C techniques. These NOEs are extremely sensitive to local conformation, and are critical to the eventual determination of a 3D structure; using these NOEs to assign resonances in the first place leads to circular reasoning. The 100% abundant ^{31}P nucleus is ideally positioned between (deoxy)ribose units, and is usually J-coupled to protons of both neighbors. ^{31}P–^{1}H correlation by heteroTOCSY offers the possibility of unambiguous sequential assignments based solely on through-bond effects, as demonstrated in Fig. 5.

The heteroTOCSY approach can be compared with other possible methods of ^{31}P–^{1}H correlation for proton assignments. The proton-detected hetero-COSY experiment of Fig. 2 is quite sensitive, but the antiphase multiplet structure reduces the resolution in both dimensions and also attenuates some cross peaks (Sklenar et al., 1986). Proton-excited/-detected experiments such as HMQC and HSQC, which have proven so powerful for ^{13}C–^{1}H and ^{15}N–^{1}H correlation in proteins (Bax et al., 1989), are not as advantageous for ^{31}P–^{1}H correlation in nucleic acids (Byrd et al., 1986). The long delays necessary for complete refocusing of heteronuclear couplings damp any sensitivity gain from proton excitation, a gain minimized anyway by the high inherent

TABLE 2
BACKBONE PROTON ASSIGNMENTS IN d(CGCGAATTCGCG)$_2$ AT 303 K

Residue	Chemical shift of deoxyribose proton (ppm)		
	H3'	H4'	H5',H5"
dC1	4.68	4.04	3.82
dG2	4.93	4.31	4.04/3.94
dC3	4.77	4.14	4.09
dG4	4.95	4.28	4.04/3.96
dA5	5.02	4.41	4.18/4.15
dA6	4.96	4.42	4.23
T7	4.78	4.15	4.09/4.06
T8	4.86	4.17	4.07
dC9	4.83	4.11	4.11
dG10	4.95	4.33	4.10/4.03
dC11	4.77	4.15	4.11
dG12	4.64	4.13	4.03

All chemical shifts are taken from the 3D heteroTOCSY-NOESY experiment and are given relative to DSS.

sensitivity of the ^{31}P nucleus. Similarly, the COLOC and DOC methods advocated by Gorenstein rely on delays adjusted for a narrow range of coupling constants (Fu et al., 1988; Jones et al., 1988). This can be advantageous in some circumstances, but our goal here is bulk polarization transfer to protons, both for observation and also for further manipulation.

Why do we observe sequential ^{31}P–^{1}H correlations in the heteroTOCSY spectrum?

The sequential, through-bond correlation of backbone resonances (Fig. 5) suggests a ^{31}P-driven backbone resonance assignment strategy which does not depend on the appearance of sequential NOEs predicted from structural models. Such a strategy does depend on nucleic acid conformation, however, because ^{31}P–^{1}H coupling constants vary widely with backbone conformation. For example, sequential connectivities were not observed in the heteroTOCSY spectrum of a double-stranded RNA oligonucleotide of similar complexity to the DNA dodecamer (Kellogg, 1992a). In principle, this and other differences can be accounted for. The rates of transfer during cross-polarization depend on the magnitudes of the relevant coupling constants, which are themselves a function of molecular geometry. However, paradoxically, of the common DNA sugar pucker geometries, the idealized B-form (C2'-endo, pseudorotation phase angle P = 162°) has the smallest H3'–H4' coupling constant, around 1 Hz. Since coherence transfer via this coupling is essential for the observation of sequential ^{31}P–H3' correlations, one might expect B-form helices to be the *least* likely of all common geometries to give sequential correlations.

This prediction is supported by simulation of the time course of coherence transfer through spin systems corresponding to different sugar pucker geometries. We ran simulations of a heteroTOCSY experiment on model dinucleotides (see Materials and Methods), starting with B-form deoxyribose and backbone geometry, and adjusting the pseudorotation phase angle in regular steps of 36°. Minimal sequential H3' transfer is predicted for deoxyribose sugars in the C2'-endo conformation, even after long mixing times, while stronger sequential transfer is predicted for all of the other (C1'-exo, O-endo, C4'-exo, C3'-endo) geometries (Fig. 7A). These simulations indicate that perfect C2'-endo B DNA should not give sequential H3' correlations in a heteroTOCSY spectrum. The simulations do not indicate why sequential H3' correlations are observed in $d(CGCGAATTCGCG)_2$, or why they are not observed in an A-form RNA double helix. To address the influence of backbone geometry on sequential transfer, we ran a set of simulations starting from a perfect A-form helix. If the A-form backbone geometry is used for simulations, otherwise identical to those of Fig. 7A, then the magnitude and rate of sequential H3' transfer drops dramatically for all pseudorotation angles (Fig. 7B). Intranucleotide transfer is correspondingly increased (not shown).

Neither perfect B-form nor A-form helices should give rise to sequential ^{31}P–H3' correlations in a heteroTOCSY, but for different reasons. In a perfect C2'-endo (B form) geometry, the small $^{3}J_{3'-4'}$ blocks sequential transfer, but a significant population of any intermediate pseudorotation geometry increases the likelihood of observable sequential correlations. The backbone geometries of A and B helices differ most at the ε angle, resulting in a much larger scalar coupling between ^{31}P and H3' in the A form (ca. 9.4 Hz) than in the B form (ca. 4.1 Hz). In the perfect A form, rapid transfer of coherence from each ^{31}P to the preceding residue limits the availability of coherence for sequential transfer to the following residue. This 'coherence siphoning' effect should damp sequential ^{31}P–H3' correlations in a heteroTOCSY whenever $^{3}J_{P-H3'}$ is much larger than the sum of ^{1}H–^{31}P couplings to the following residue, regardless of the phase angle of pseudorotation.

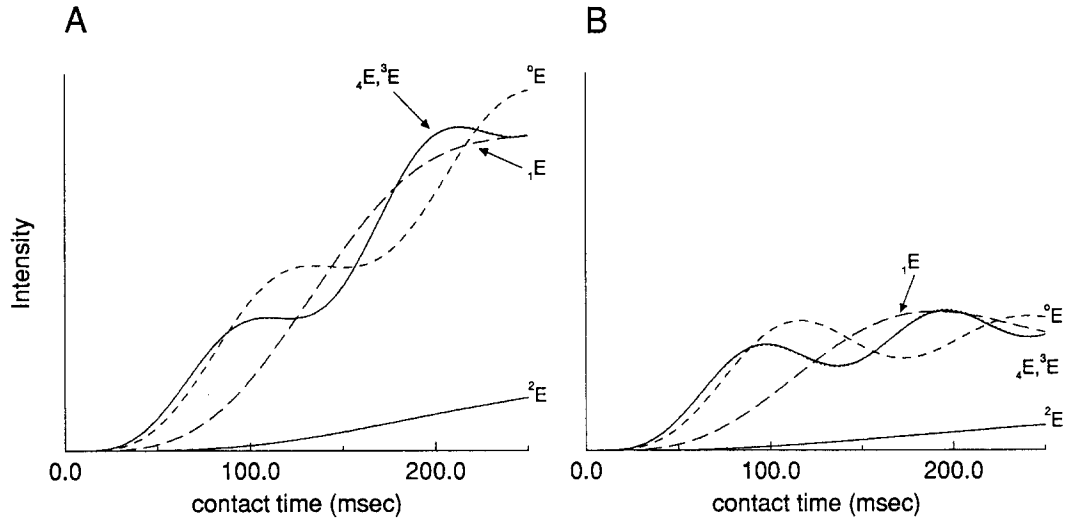

Fig. 7. Simulation of the time dependence of coherence transfer in dinucleotide models. Curves represent observable magnetization, predicted for the H3' nucleus on the second sugar in a dinucleotide, i.e., 5'-NpN-3'. Input parameters are generated as described in Materials and Methods. (A) B-form backbone geometry with varying pseudorotation. Curves are marked as ^2E (C2'-endo, P = 162°), $_1E$ (C1'-exo, P = 126°), ^0E (O-exo, P = 90°), $_4E$ (C4'-endo, P = 54°), and ^3E (C3'-endo, P = 18°). (B) A-form backbone geometry with varying pseudorotation angle. The notation is the same as in part A; these figures differ only in the backbone coupling constants.

The fact that we see H3' interresidue correlations implies that deoxyribose geometries other than pure C2'-endo occur in $d(CGCGAATTCGCG)_2$, a possibility that has been addressed by solution NMR and theoretical studies. Two-dimensional PE-COSY (Bax and Lerner, 1988) and DQF-COSY (data not shown) experiments on this molecule indicate that the H3'–H4' coupling constants are significant, averaging in the range typical of C1'-exo deoxyribose puckering. Nerdal et al. (1989) published a distance-geometry structure of $d(CGCGAATTCGCG)_2$ refined by back-calculation of NOESY spectra; their data did not include any coupling constant information, and they present only a single structure, refined with back-calculation. Deoxyribose pseudorotation in the structure of Nerdal et al. varies widely, from a southwestern extreme of 251° (4'-endo-O-exo) for dG2 to an eastern extreme of 91° (O-endo) for dG10.

Bax and Lerner interpreted their data in terms of a rapid north-south pseudorotational equilibrium, with N populations as high as 25%, and an S pseudorotation angle averaging 132°, very near C1'-exo. Nerdal et al. interpreted their data as a single underwound structure with unusual pseudorotation and backbone angles. Others have presented NMR evidence for unexpected pseudorotation phase angles in double-helical DNA oligonucleotides, with a variety of interpretations. For example, Hosur et al. (1986) suggest pseudorotation phase angles ranging from O-endo to C1'-exo for $d(GAATTCGAATTC)_2$, Chary et al. (1989) claim O-endo in $d(ACATCGATGT)_2$, and Kim et al. (1992) claim C1'-exo for pyrimidines, and sugar conformations closer to C2'-endo for internal purines, in $d(CGCGTTAACGCG)_2$. Gochin et al. (1990), in a detailed study of the alternating purine-pyrimidine tract $d(AC)_4 \cdot d(GC)_4$, discuss both single-conformer and two-state structural models that could be used to fit their data.

A structural model for $d(CGCGAATTCGCG)_2$ based on ca. 100% C2'-endo pseudorotation is

untenable, but a choice between the proposed models cannot be made on the basis of hetero-TOCSY spectra alone. Clearly, models that incorporate data from coupling constant analysis are preferred to models that do not. However, the interpretation of coupling constants is itself problematic when made in the context of a dynamic equilibrium. The H3'–H4' coupling constant is a prime example. Its value is at a minimum near true south on the pseudorotation cycle, and at a maximum near true north. In a two-state model, a measured value higher than the possible minimum is taken to indicate a small population of 3'-endo (northern) conformers in an population dominated by 2'-endo (southern) conformers (Rinkel and Altona, 1987). In a single-state model, such a coupling constant is taken directly as an indicator of average conformation. If, say, the actual population is a distribution of conformations ranging over the southern half of the pseudorotation cycle, the measured value of $^3J_{3'-4'}$ is an intermediate one, even if the average conformation is 2'-endo and the northern half of the cycle is insignificantly populated. In such a case, neither a two-state nor a static model accurately reflects the physical situation and a set of interrelated coupling constants is best interpreted simultaneously, with a range of possible models in mind. We consider the comment of Gochin et al. (1990), that 'analysis in terms of a two-state model simply reminds us that there is in reality a dynamic conformational equilibrium', worth remembering.

The sequential correlations in 2D heteroTOCSY-NOESY

Whereas in RNA, sequential cross peaks were observed in the ^{31}P–^1H aromatic region of a heteroTOCSY-NOESY spectrum, in the DNA molecule studied here the correlations in that region are quite weak. We suspect that this difference is due to the proximity of the H2' proton of each ribose in A-form RNA to the aromatic proton of the subsequent residue, resulting in a large sequential NOE. Intranucleotide aromatic NOEs in RNA are enhanced by the efficient transfer of ^{31}P coherence to the intranucleotide H3' proton. In RNA, both aromatic correlations probably originate not only from the same ^{31}P nucleus, but from ^1H coherence on the same sugar.

We note, however, the presence of a complete set of sequential and intranucleotide cross peaks in the ^{31}P–^1H anomeric region of the DNA spectrum, in contrast to the weaker sequential cross peaks observed in the heteroTOCSY-NOESY spectrum of RNA (Kellogg et al., 1992). The sequential anomeric cross peaks in the spectra of DNA are enhanced by stronger sequential heteroTOCSY transfer of magnetization to H4', which is then close to the anomeric proton. The heteroTOCSY-NOESY experiment also provides nearly complete ^{31}P–^1H correlations in the H2'/H2" region in DNA; severe overlap of the H2', H3', H4' and H5'/H5" resonances in RNA spectra prevents the full resolution of these useful correlations.

Three-dimensional heteronuclear NMR without isotopic labeling

As shown in Fig. 6 and Table 2, a 3D version of the heteroTOCSY-NOESY experiment improves the resolution in the ^1H dimension sufficiently to assign unambiguously entire deoxyribose proton spin systems, including H5' and H5" resonances. This improvement is analogous to the improved resolution in ^{15}N- and ^{13}C-separated homonuclear experiments (Fesik and Zuiderweg, 1988; Marion et al., 1989).

One of the most striking (but expected) features of the 3D spectrum is the strength of intranucleotide NOEs. Peaks at a given H3' frequency in ω_2 consistently show correlations to H4', H5' and H5" protons of the same sugar in ω_3, which are correlated with each other in an ω_2–ω_3 plane.

Likewise, H4', H5' and H5" peaks in ω_2 show the reverse correlations. Each phosphorus is scalarly coupled to two adjacent deoxyribose spin systems; thus, the repeated pattern of intranucleotide NOEs on different phosphorus planes permits a sequential walk along the chain. The narrow sweep width in the ^{31}P dimension enables collection of high-resolution data in all three dimensions.

H5'/H5" proton assignments of this DNA duplex have been obtained previously using homonuclear TOCSY experiments with a long (500 ms) mixing time (Glaser et al., 1989). A comparison of their H5'/H5" assignments with those given in Table 2 reveals a number of small ($\leq$ 0.03 ppm) differences. While these differences approach the limit of digital resolution, we believe that the assignments obtained by the ^{31}P-separated ^1H–^1H NOESY experiment are less ambiguous than those from TOCSY data. The 3D experiment also avoids some of the problems, such as sample heating and propagation of random phase errors, inherent in TOCSY experiments with lengthy mixing periods.

Homonuclear 3D experiments have also been applied to nucleic acids with considerable promise. Piotto and Gorenstein (1991) used a homonuclear 3D NOESY-TOCSY experiment to obtain deoxyribose assignments for the GG mismatch dodecamer d(CGGGAATTCGCG)$_2$. In Fig. 2 of that study, slices perpendicular to the aromatic proton resonances are reported to show resolved cross peaks to H5' and H5" resonances. No H4' cross peak is shown, however, suggesting that either the peaks labeled H5' and H5" are actually H4' peaks, or H4' and H5'/H5" cross peaks are not resolved in this experiment. We suspect that the latter is true, because we have been unable to obtain the resolution necessary to separate H4' and H5'/H5" cross peaks using 3D NOESY-TOCSY experiments on our dodecamer (data not shown). Mooren et al. (1991) applied a homonuclear 3D TOCSY-NOESY experiment to a 15-mer DNA hairpin and present a figure where all the deoxyribose protons for one residue are clearly resolved; no assignments for other residues are given.

The 3D heteroTOCSY-NOESY experiment is proton detected, but relies on the sensitivity of ^{31}P for excitation. Three-dimensional homonuclear and most 3D heteronuclear experiments have the strength of both proton excitation and detection, and are thus inherently more sensitive. However, nonselective homonuclear 3D experiments have a far greater number of cross peaks than homonuclear 2D experiments, and it is time consuming to collect high-resolution data in all three dimensions. The 3D heteronuclear experiment simplifies ^1H–^1H spectra by editing in the X (^{31}P) dimension, and the indirectly detected frequency dimensions are sufficiently narrow to permit collection of high-resolution data in a reasonable period of time. If collection time and spectrometer stability are not limiting factors, more scans can be collected for increased sensitivity.

CONCLUSIONS

Heteronuclear 3D NMR is completely feasible for unlabeled nucleic acids, using the naturally occurring ^{31}P resonance as the heteronuclear label. The strategy described here, combining 2D and 3D ^{31}P–^1H experiments, bears as much resemblance to ^1H homonuclear methods as to ^{13}C–^1H and ^{15}N–^1H heteronuclear methods. The simplification of proton spectra by addition of a third dimension is analogous to other heteronuclear methods. However, like homonuclear 3D experiments, the experimental sensitivity is likely to decrease for large oligonucleotides, due to more

rapid transverse relaxation of both nuclei. For NMR spectroscopy of RNA, an area where a great deal of attention is being directed, the upper limit of this approach will probably be increased by ^{13}C labeling of the ribose. With ^{13}C labeling, ^{1}H-detected ^{31}P–^{13}C heteroTOCSY experiments are possible, utilizing the large one-bond ^{13}C–^{13}C coupling for subsequent transfer steps.

We have not explored sequence-specific variations in molecular geometry and their influence on the coherence transfer functions for nucleic acids, although such an approach might prove fruitful. Indeed, our results strongly suggest that sequence-specific effects are operative in determining coherence transfer efficiency. A good example of this are the markedly weaker ^{31}P–^{1}H cross peaks seen for residue dA6 in all regions of the spectrum. In this study, we have tried to provide a basis for interpretation of data from this new class of experiments, and to establish a working basis for sequential assignment of backbone resonances of nucleic acids, even in the absence of information about other resonances. Of course, in most cases other information will be available, and this approach will dovetail with established and emerging methods for complete assignment of nucleic acid spectra.

Note added in proof

In a personal communication from Dr. David Gorenstein (Purdue University), it was pointed out that in the 3D NOESY-TOCSY experiment described in Piotto and Gorenstein (1991), the lack of a H6–H4' cross peak is likely to be due to the greater distance between this proton pair compared to the H6–H5'/H5" protons, and not to incorrect assignment as suggested in the present paper.

ACKNOWLEDGEMENTS

We are deeply indebted to Prof. Peter B. Moore for his support and criticism at all stages of this work, and for his careful reading of the manuscript. We thank Mr. Peter Demou for his modifications to the spectrometer, and for his years of dedicated service to Yale University. We also thank Prof. Gary Drobny (University of Washington) and Mr. Alex Szewczak (Yale) for their comments. B.I.S. is supported by National Research Service Award F32 AI08472 and by ACS Institutional Research Grant IN31-33. G.W.K. is supported by NIH grant GM-41651 to Peter B. Moore (Department of Chemistry). NMR and additional computational facilities were supported by the NIH (RR03475), the NSF (DMB8610557), and the American Cancer Society (RD259).

REFERENCES

Altona, C. (1982) *Recl. Trav. Chim. Pays-Bas*, **101**, 412–433.
Arnott, S., Chandrasekeharan, R., Birdsall, D.L., Leslie, A.G.W. and Ratcliffe, R.L. (1980) *Nature*, **283**, 743–745.
Artemov, D.Y. (1991) *J. Magn. Reson.*, **91**, 405–407.
Bax, A. and Davis, D.G. (1985) *J. Magn. Reson.*, **65**, 355–360.
Bax, A. and Lerner, L. (1988) *J. Magn. Reson.*, **79**, 429–438.
Bax, A., Sparks, S.W. and Torchia, D.A. (1989) *Methods Enzymol.*, **176**, 134–150.
Bearden, D.W. and Brown, L.R. (1989) *Chem. Phys. Lett.*, **163**, 432–436.
Braunschweiler, L. and Ernst, R.R. (1983) *J. Magn. Reson.*, **53**, 521–528.
Byrd, R.A., Summers, M.F., Zon, G., Fouts, C.S. and Marzilli, L.G. (1986) *J. Am. Chem. Soc.*, **108**, 504–505.
Cavanagh, J., Chazin, W.W. and Rance, M. (1990) *J. Magn. Reson.*, **87**, 110–131.
Chary, K.V.R., Hosur, R.V. and Govil, G. (1989) *Biochemistry*, **27**, 3858–3867.

Clore, G.M. and Gronenborn, A.M. (1985) *FEBS Lett.*, **199**, 187–198.
Connolly, B.A. and Eckstein, F. (1984) *Biochemistry*, **23**, 5523–5527.
Feigon, J., Leupin, W., Denny, W.A. and Kearns, D.R. (1983) *Biochemistry*, **22**, 5943–5951.
Fesik, S.W. and Zuiderweg, E.R.P. (1988) *J. Magn. Reson.*, **78**, 588–593.
Field, L.D. and Messerle, B.A. (1985) *J. Magn. Reson.*, **62**, 453–460.
Field, L.D. and Messerle, B.A. (1986) *J. Magn. Reson.*, **66**, 483–490.
Fu, J.M., Schroeder, S.A., Jones, C.R., Santini, R. and Gorenstein, D.G. (1988) *J. Magn. Reson.*, **77**, 577–582.
Glaser, S.J., Remerowski, M.L. and Drobny, G.P. (1989) *Biochemistry*, **28**, 1483–1492.
Gochin, M., Zon, G. and James, T.L. (1990) *Biochemistry*, **29**, 11161–11171.
Gorenstein, D.G., Schroeder, S.A., Fu, J.M., Metz, J.T., Roongta, V. and Jones, C.R. (1988) *Biochemistry*, **27**, 7223–7237.
Hare, D.R., Wemmer, D.E., Chou, S., Drobny, G. and Reid, B.R. (1983) *J. Mol. Biol.*, **171**, 319–336.
Haasnoot, C.A.G., De Leeuw, F.A.A.M. and Altona, C. (1980) *Tetrahedron*, **36**, 2783–2792.
Hiroaki, H. and Uesugi, S. (1989) *FEBS Lett.*, **244**, 43–46.
Hosur, R.V., Ravikumar, M., Chary, K.V.R., Sheth, A., Govil, G., Zu-Kun, T. and Miles, H.R. (1986) *FEBS Lett.*, **205**, 71–76.
Jones, C.R., Schroeder, S.A. and Gorenstein, D.G. (1988) *J. Magn. Reson.*, **80**, 370–374.
Kellogg, G.W. (1992a) *J. Magn. Reson.*, **98**, 176–182.
Kellogg, G.W. (1992b) *J. Magn. Reson.*, **97**, 623–627.
Kellogg, G.W., Szewczak, A.A. and Moore, P.B. (1992) *J. Am. Chem. Soc.*, **114**, 2727–2728.
Kim, S.-G., Line, L.-J. and Reid, B.R. (1992) *Biochemistry*, **31**, 3564–3574.
Marion, D. and Lancelot, G. (1984) *Biochem. Biophys. Res. Commun.*, **124**, 774–783.
Marion, D. and Wüthrich, K. (1983) *Biochem. Biophys. Res. Commun.*, **113**, 967–974.
Marion, D., Kay, L.E., Sparks, S., Torchia, D. and Bax, A. (1989) *J. Am. Chem. Soc.*, **111**, 1515.
Metzler, W.J., Wang, C., Kitchen, D., Levy, R.M. and Pardi, A. (1990) *J. Mol. Biol.*, **214**, 711–736.
Mooren, M.M.W., Hilbers, C.W., Van der Marel, G.A. and Van Boom, J.H. (1991) *J. Magn. Reson.*, **94**, 101–111.
Morris, G.A. and Gibbs, A. (1991) *J. Magn. Reson.*, **91**, 444–449.
Müller, L. and Ernst, R.R. (1979) *Mol. Phys.*, **38**, 963–992.
Nerdal, W., Hare, D.R. and Reid, B.R. (1989) *Biochemistry*, **28**, 10008–10021.
Nikonowicz, E.P. and Pardi, A. (1992a) *J. Am. Chem. Soc.*, **114**, 1082–1083.
Nikonowicz, E.P. and Pardi, A. (1992b) *Nature*, **355**, 184–186.
Nilges, M., Clore, G.M., Gronenborn, A.M., Brunger, A.T., Karplus, M. and Nilsson, L. (1987) *Biochemistry*, **26**, 3718–3733.
Ott, J. and Eckstein, F. (1985) *Biochemistry*, **24**, 2530–2535.
Otting, G., Widmer, H., Wagner, G. and Wüthrich, K. (1985) *J. Magn. Reson.*, **66**, 187–193.
Pardi, A., Walker, R., Rapoport, H., Wider, G. and Wüthrich, K. (1983) *J. Am. Chem. Soc.*, **105**, 1652.
Pardi, A. and Nikonowicz, E.P. (1992) *J. Am. Chem. Soc.*, **114**, 9202–9203.
Piotto, M.E. and Gorenstein, D.G. (1991) *J. Am. Chem. Soc.*, **113**, 1438–1440.
Reid, B.R. (1987) *Quart. Rev. Biophys.*, **20**, 1–34.
Rinkel, L.J. and Altona, C. (1987) *J. Biomol. Struct. Dyn.*, **4**, 621–649.
Roongta, V.A., Jones, C.R. and Gorenstein, D.G. (1990) *Biochemistry*, **29**, 5245–5258.
Schroeder, S.A., Fu, J.M., Jones, C.R. and Gorenstein, D.G. (1987) *Biochemistry*, **26**, 3812–3821.
Shaka, A.J. (1988) *J. Magn. Reson.*, **77**, 274–280.
Scheek, R.M., Boelens, R., Russo, N., Van Boom, J.H. and Kaptein, R. (1984) *Biochemistry*, **23**, 1371–1376.
Sklenar, V., Miyashiro, H., Zon, G., Miles, H.T. and Bax, A. (1986) *FEBS Lett.*, **208**, 94–98.
Sklenar, V. and Bax, A. (1987) *J. Am. Chem. Soc.*, **109**, 7525–7526.
States, D.J., Haberkorn, R.A. and Ruben, D.J. (1982) *J. Magn. Reson.*, **48**, 286–292.
Van de Ven, F.J.M. and Hilbers, C.W. (1988) *Eur. J. Biochem.*, **178**, 1–38.
Van Wijk, J., Huckriede, B.D., Ippel, J.H. and Altona, C. (1992) *Methods Enzymol.*, **211**, 286–306.
Varani, G. and Tinoco Jr., I. (1991) *Quart. Rev. Biophys.*, **24**, 479–532.
Wüthrich, K. (1986) *NMR of Proteins and Nucleic Acids*, Wiley, New York.
Zagorski, M.G. and Norman, D.G. (1989) *J. Magn. Reson.*, **83**, 167–172.
Zuiderweg, E.R.P. (1990) *J. Magn. Reson.*, **89**, 533–542.